The Journal of Immunology

RESEARCH ARTICLE | MAY 15 2014

Characterization of Platelet–Monocyte Complexes in HIV-1–Infected Individuals: Possible Role in HIV-Associated Neuroinflammation FREE

Meera V. Singh; ... et. al

J Immunol (2014) 192 (10): 4674–4684.
https://doi.org/10.4049/jimmunol.1302318

Characterization of Platelet–Monocyte Complexes in HIV-1–Infected Individuals: Possible Role in HIV-Associated Neuroinflammation

Meera V. Singh,* Donna C. Davidson,* Joseph W. Jackson,* Vir B. Singh,* Jharon Silva,* Servio H. Ramirez,† and Sanjay B. Maggirwar*

HIV-1–associated neuroinflammation persists even with effective combined antiretroviral therapy, and it is associated with the presence of activated monocytes/macrophages within the CNS. To infiltrate the CNS, monocytes transmigrate across the selectively permeable blood–brain barrier, which is compromised during HIV-1 infection. Interestingly, platelet-derived excess soluble CD40 ligand found in the plasma and cerebrospinal fluid of HIV-1–infected individuals with cognitive impairment has previously been implicated in increased blood–brain barrier permeability. In this study we show that soluble CD40 ligand also promotes the formation of complexes between inflammatory monocytes and activated platelets (PMCs), which are detected by flow cytometry as monocytes that express excess of CD61, a platelet marker, and that these complexes are increased in individuals with HIV-1 infection. PMCs exhibit an enhanced ability to adhere to human brain microvascular endothelial cells as compared with monocytes alone, and they migrate across the transendothelial barrier. These complexes can be found marginalized in the lumen of postcapillary venules in postmortem brain tissue derived from cases of HIV-1–associated encephalitis. The extravasation of monocytes across the brain endothelium may exacerbate neuroinflammation, indicating that enhancing this event via platelet interaction may be a contributing factor in the development of cognitive impairment. Thus, dampening platelet activation, and in turn PMC formation, with antiplatelet agents may prove beneficial in developing adjunctive therapies for use in combination with combined antiretroviral therapy in an effort to reduce HIV-1–associated neurologic deficit. ***The Journal of Immunology*****, 2014, 192: 4674–4684.**

Human immunodeficiency virus type 1 (henceforth referred to as HIV-1) enters the CNS during the acute phase of infection (1) via infected monocytes, which upon entry into the CNS differentiate into macrophages, thus allowing viral infection to persist primarily in perivascular macrophages and microglia (reviewed in Ref. 2). In certain cases, HIV-1 infection in the brain can develop into a neuropathology known as HIV-1–associated encephalitis (HIV-E), which is comprised of microglial nodules, activated resident microglia, multinucleated giant cells, infiltration predominantly by monocytoid cells including blood-derived macrophages, and distinct neuronal loss (3). Clinically, HIV-1 infection in the CNS can manifest as a spectrum of disorders collectively known as HIV-1–associated neurocognitive disorders (HAND). In the post–antiretroviral treatment (ART) era, the incidence of the most severe form of HAND, HIV-1–associated dementia, has dramatically decreased; however, >50% of HIV^+ patients continue to suffer from milder versions of HAND (4).

Because neurons are not productively infected with HIV-1, other pathological mechanisms have been implicated in neuronal damage and death that occur during HIV-E. Indeed, changes in the brain microenvironment are thought to occur as a consequence of an overwhelming inflammatory response, involving overstimulation and excitotoxicity, induced either by viral proteins such as Tat, gp120, and Vpr or by proinflammatory host factors secreted from microglia and macrophages, such as TNF-α, MCP-1, and platelet-activating factor (5, 6). Interestingly, clinical signs of HAND are more closely associated with increased numbers of activated microglia and infiltrating monocytes rather than the viral load within the CNS (7, 8).

Human monocytes are classified into two subtypes based on the expression of CD16. Classical monocytes are $CD14^+CD16^-$ and comprise 80–90% of all circulating monocytes, whereas $CD14^+$ $CD16^+$ monocytes represent 5–10% of the monocyte population under normal conditions and are considered to be a more mature and proinflammatory subset (reviewed in Ref. 9). Consistently, $CD16^+$ monocytes are expanded up to 40% during HIV-1 infection (10) and are more susceptible to infection than $CD16^-$ monocytes (11). These cells are also the most abundant subtype of monocyte found within the CNS during HIV-1 infection (12), and their expansion in the blood might be predictive of HIV-1–associated neuroinflammation (13, 14). $CD16^+$ monocytes also exhibit an enhanced capacity for migration across endothelial barriers, attributable to increased expression of integrins such as $\alpha_4\beta_1$ and $\alpha_M\beta_2$

*Department of Microbiology and Immunology, University of Rochester Medical Center, Rochester, NY 14642; and †Department of Pathology and Laboratory Medicine, Temple University School of Medicine, Philadelphia, PA 19140

Received for publication August 29, 2013. Accepted for publication March 6, 2014.

This work was supported by National Institutes of Health Grants R01 NS054578, R01 NS066801 (to S.B.M.), and T32 AI049815 (to J.W.J.). This work was also supported by the Rochester Center for AIDS Research (National Institutes of Health Grant P30 AI078498).

The funder had no role in study design, data collection and analysis, decision to publish, or preparation of the manuscript.

Address correspondence and reprint requests to Prof. Sanjay B. Maggirwar, Department of Microbiology and Immunology, University of Rochester Medical Center, 601 Elmwood Avenue, Box 672, Rochester, NY 14642. E-mail address: sanjay_maggirwar@urmc.rochester.edu

Abbreviations used in this article: ART, antiretroviral therapy; BBB, blood–brain barrier; BMVEC, brain microvascular endothelial cell; cART, combined antiretroviral therapy; HAND, HIV-1–associated neurocognitive disorder; HIV-1, HIV type 1; HIV-E, HIV-1–associated encephalitis; PMC, platelet–monocyte complex; PSGL-1, P-selectin glycoprotein ligand 1; rh, recombinant human; rm, recombinant mouse; sCD40L, soluble CD40L; VNR, vitronectin receptor.

(15), that mediate adherence to endothelial cells, and chemokine receptors such as CX3CR1, which increase responsiveness to fractalkine (16).

Previous reports have shown that the $CD16^+$ phenotype is also induced by the interaction of monocytes with activated platelets. Activated platelets form transient complexes with monocytes in circulation, termed platelet–monocyte complexes (PMCs), and these complexes are elevated in diseases involving inflammation such as cardiovascular disease (17) and type 2 diabetes (reviewed in Ref. 18). Interestingly, PMCs were found to be a more sensitive marker of platelet activation and predictor of myocardial infarction as compared with levels of P-selectin, also known as CD62P, which is the traditional hallmark of platelet activation (19). Moreover, the extent to which PMCs develop is predominantly dependent on the platelet activation status (20, 21), and only to a very limited extent on monocyte activation (22).

Previous studies from our group (21) and others (23) have demonstrated that HIV-1 infection induces an increase in platelet activation, despite thrombocytopenia. Infection, as well as cognitive impairment during infection, is associated with an increase in plasma levels of soluble CD40 ligand (sCD40L) (24), for which platelets are the major source (25). Consistent with this notion, recent reports from our group indicate that excess sCD40L contributes to blood–brain barrier (BBB) permeability in the context of HIV-1 (26), and that PMCs are elevated in individuals with HIV-1 infection despite suppressive combined ART (cART) (21). Collectively, these findings underscore the importance of PMCs in the pathogenesis of HIV-1–associated illnesses, and they led us to the underlying hypothesis that during HIV-1 infection, the increase in platelet activation and subsequent release of sCD40L promote the formation of PMCs, which in turn have a higher propensity to cross the BBB, thereby exacerbating HIV-1–associated neuroinflammation.

The findings in the present study indicate that HIV-1–infected individuals exhibit increased levels of PMCs as compared with uninfected individuals, and that sCD40L activates platelets in a manner that promotes the formation of complexes with monocytes via engagement of P-selectin and P-selectin glycoprotein ligand 1 (PSGL-1) on platelets and monocytes, respectively. Consistently, mice treated with CD40L also exhibit a significant increase in $Gr\text{-}1^{hi}$ (the functional equivalent of $CD16^+$ monocytes in humans) inflammatory monocyte complexes as compared with saline-treated mice. Using an in vitro coculture system, as well as brain specimens derived from individuals with HIV-E, we now reveal that monocyte extravasation into the CNS is accentuated by the increased adherence of PMCs to brain microvascular endothelial cells. Importantly, we also show that these complexes can be detected as marginalized to the vessel lumen and in perivascular cuffs in brain tissue derived from individuals with HIV-E. Taken together, these results shed light on the underlying mechanisms that may contribute to the pathogenesis of neuroinflammation and HIV-E, thus revealing novel therapeutic targets. Currently, there remains a critical lack of adjunctive therapies for the management of HIV-1–associated neurocognitive disorders; however, without addressing the underlying neuroinflammation, no realistic control of these complications can be achieved.

Materials and Methods

Ethics statement

The Research Subjects Review Board at the University of Rochester Medical Center approved studies involving human samples. All study participants were adults and blood samples were obtained after written informed consent, in accordance with the Declaration of Helsinki. Mouse experiments were carried out in accordance with the Animal Welfare Act and the National Institutes of Health (NIH) guidelines, and the University Committee on Animal Resources of the University of Rochester Medical Center approved the animal protocol (protocol no. 2005-161). The facilities and programs of the Vivarium and Division of Laboratory Animal Medicine of the School of Medicine and Dentistry are fully accredited by the Association for the Assessment and Accreditation of Laboratory Animal Care International.

Patient samples

Persons with (n = 36) and without (n = 37) HIV-1 infection (without any occurrence of cardiovascular disease for at least one preceding year) were enrolled in the study, and blood samples were drawn into acid citrate dextrose–buffered vacutainers (BD Biosciences, San Jose, CA). All persons with HIV-1 infection were on ART at the time of the draw. Six of the HIV-1–infected individuals were coinfected with hepatitis C, one was infected with tuberculosis, and one was infected with human papillomavirus. Patient demographics are as outlined in Table I.

Flow cytometry and ImageStream analysis

PMCs were detected in whole blood, using a previously described method (21), within 1 h of the blood draw. In brief, 100 μl blood was fixed and RBCs were lysed and then stained with 10 μl anti–CD14-PE, 3 μl anti–CD16-PE-Cy7, 10 μl anti–CD62P FITC (all obtained from BD Biosciences, San Jose, CA), and 3 μl anti–CD61-Alexa Fluor 647 (from AbD Serotec, Oxford, U.K.). Following the staining, samples were acquired using a flow cytometer (Accuri C6; Accuri Cytometers, Ann Arbor, MI). Whole blood leukocytes and monocytes were gated based on forward and side scatter. Further monocytes ($CD14^+$ cells) were divided into two subtypes based on CD16 expression. PMCs were defined as monocytes that were positive for CD61, a platelet-specific marker. The same tubes were also analyzed for platelet activation using CD62P (also known as P-selectin) expression. Fluorescence minus one controls were used to define various gates, and sizing beads (Mega Mix; BioCytex, Marseille, France) were used to delineate the platelet gate (0.9–3 μm).

Representative samples from HIV^+ (n = 5) and HIV^- (n = 6) donors were also acquired and analyzed using ImageStream (Amnis, Seattle, WA). For these studies, 10 μl anti–CD16-Pac B (from BD Biosciences) was used in place of anti–CD16–PE-Cy7. Ideas software (Amnis) was used to analyze the ImageStream data. The gating strategy used was as described above. Initial analysis of the data indicated two types of PMCs: one in which platelets were attached to the surface of monocytes (henceforth called type 1 complexes), and another in which there was no visible platelet attached, but the monocyte itself expressed the platelet marker CD61 (henceforth called type 2 complexes). The internalization feature of the Ideas software, which measures and plots the distance between fluo-

Table I. Demographic and clinical characteristics of study participants

Characteristics	HIV^-	HIV^+
Mean age ± SD, y	34 ± 13	48 ± 13
Race, *N* (%)		
Black	3 (7)	24 (51)
White	38 (86)	15 (32)
Hispanic	1 (2)	3 (6)
Unspecified	2 (5)	5 (11)
Gender, *N* (%)		
Male	24 (55)	36 (78)
Female	20 (45)	11 (22)
Drug Use, *N* (%)		
No.	43 (98)	21 (45)
Cocaine	1 (2)	11 (24)
Marijuana	0 (0)	12 (26)
Heroin	0 (0)	2 (4)
Nicotine	0 (0)	0 (0)
Alcohol	1 (2)	8 (17)
Mean CD4 Count ± SD, Cells/mm^3	NA	585 ± 240
Viral Load		
Undetectable, *N* (%)	NA	26 (57)
Detectable, Mean ± SD, RNA Copies/ml	NA	128 ± 132

Individuals with (n = 36) and without (n = 37) HIV-1 infection were enrolled in the study. All HIV-1–infected individuals were on ART. Six HIV^+ individuals were coinfected with hepatitis C, one with tuberculosis, and one with human papillomavirus. Unless otherwise stated, the values indicate numbers with the percentage of total study population in parentheses.

rochromes of interest (i.e., CD14 for monocytes and CD61 for platelets) was used to differentiate between these two types of complexes and to measure the relative percentage of these two types among the total PMC population. Additionally, the spot count feature was used to measure the number of platelets per monocyte in a complex. This feature measures pixel intensity of a particular fluorochrome after subtracting the background (in this case CD61 expression on monocytes) and examines whether this connects to a particular spot on the image (i.e., a platelet).

Cell culture

Monocytes were isolated using a MACS Pan Monocyte Isolation Kit (Miltenyi Biotec, San Diego, CA) as per the manufacturer's instructions with minor modifications. In all experiments except for electron microscopy, biotin-labeled Ab against CD41 (250 ng/25 million PBMCs; Abcam, Cambridge, MA) was added to the Ab mixture provided with the kit to remove contaminating platelets and existing PMCs. The resulting monocytes contained <10% residual PMCs (data not shown). Monocytes used for electron microscopy contained 35–40% PMCs (data not shown). Monocytes were cultured in RPMI 1640 supplemented with 10% FBS and 2% penicillin/streptomycin/glutamine.

Whole blood from HIV^- samples was centrifuged at 250 × *g* for 15 min, and platelet-rich plasma was collected. Following addition of PGI_2 (1 μl/ml platelet-rich plasma) to maintain platelet quiescence, platelet-rich plasma was centrifuged at 1000 × *g* for 10 min to pellet the platelets. The platelet pellet was then washed and resuspended using Tyrode's salt solution (Sigma-Aldrich, St. Louis, MO) supplemented with acid citrate dextrose anticoagulant and PGI_2. Subsequently, washed platelets were centrifuged once again at 1000 × *g* for 10 min, and the remaining purified platelet pellet was resuspended in Tyrode's salt solution without supplements. The purity of isolated platelets was determined using a Sysmex KX 21N hematology analyzer and was found to be 99% pure.

Primary human brain microvascular endothelial cells (BMVECs; Applied Cell Biology Research Institute, Kirkland, WA) were cultured in DMEM/F12 supplemented with 10% FBS, 2% penicillin/streptomycin/glutamine, and 100 ng/ml endothelial cell growth supplement (BD Biosciences). Cells up to passage 10 were used for performing experiments.

Scanning electron microscopy

Monocytes isolated from the whole blood of HIV^- donors were allowed to adhere onto poly-L-lysine–coated coverslips for 2 h and were subsequently placed into 0.1 M sodium cacodylate–buffered 2.5% glutaraldehyde at 4°C for overnight fixation. The cells on the cover glasses were postfixed using the same buffer in 1.0% osmium tetroxide and then transitioned through a graded series of ethanol to 100% (×3). The last change was allowed to evaporate off of the cover glasses overnight in a fume hood. The cover glasses were then mounted onto aluminum stubs and sputter coated with gold. Imaging was performed using a Zeiss Auriga field emission scanning electron microscopy with an attached Gatan digital camera system.

Transmission electron microscopy

Monocytes were isolated, as described above, from whole blood obtained from HIV^- donors and were allowed to adhere to a two-chamber slide for 2 h, following which media was removed and immediately replaced with room temperature fixative composed of 0.1 M sodium cacodylate–buffered 2.5% glutaraldehyde. The slides were fixed for 1 h at room temperature and then at 4°C overnight. The plastic chambers were removed, and slides were rinsed in the same buffer, postfixed in 1.0% osmium tetroxide for 30 min, and then dehydrated through a graded series of ethanol to 100% (×3) concentration. The slides were then placed into a 1:1 ratio of 100% ethanol and Spurr epoxy resin for 1 h and transferred to Spurr epoxy resin overnight. The next day, size 3 BEEM capsules were filled with Spurr resin, inverted, and placed on top of the area where cells were present on the slides, and then placed into a 60°C oven to allow for overnight polymerization. The following day, glass slides/capsules were dipped three to four times in liquid nitrogen, and polymerized BEEM capsules were wiggled and "popped off" the glass. The epoxy blocks with the entrapped cells were trimmed of excess plastic resin, placed into an ultramicrotome, thin-sectioned at 70 nm onto carbon-coated nickel grids, and stained with uranyl acetate and lead citrate. Imaging was done using a Hitachi 7650 transmission electron microscope with an attached Gatan Erlangshen 11 megapixel digital camera.

Detection of PMCs in sCD40L-treated mice

C57BL/6J mice were purchased from The Jackson Laboratory (Bar Harbor, ME). Ten to 12-wk-old wild-type mice ($n = 6$/group) were injected retroorbitally with recombinant mouse (rm)sCD40L (R&D Systems, Minneapolis, MN; 0.2 μg/g body weight) that had been resuspended in saline, as previously described (26). Two hours after injection, whole blood was obtained via cardiac exsanguination and used for detection of PMCs. Two microliters anti–CD115-allophycocyanin (eBioscience, San Diego, CA), 2.5 μl CD61-Alexa Fluor 647 (AbD Serotec), 2.5 μl Gr-1-PE-Cy7, and 1 μl CD62P-FITC (BD Biosciences) were used to stain 50 μl whole blood. Samples were acquired using an Accuri C6. Fifteen thousand leukocytes per sample were collected and analyzed using FlowJo. Monocytes were gated based on CD115 expression and then classified into two subtypes using Gr-1 expression as $Gr\text{-}1^{hi}$ and $Gr\text{-}1^{lo}$, as murine monocytes expressing high levels of Gr-1 have been shown to be representative of the "inflammatory" monocyte population that corresponds to the $CD16^+$ monocyte subset within humans (9, 26). Monocytes expressing CD61 were defined as PMCs, and CD62P expression was used as a marker of platelet activation. Fluorescence minus one controls were used for analysis, as described above.

In vitro whole blood treatment with recombinant human sCD40L

Blood from HIV-1–uninfected donors ($n = 4$) was treated with either ADP at 10 μM for 30 min or with recombinant human (rh)sCD40L (R&D Systems, Minneapolis, MN) at 1 μg/ml for 2 h at 37°C. When indicated, blood was pretreated with either 8 μg/ml MK13 (neutralizing Ab against CD40L) (24) or 5 μg/ml 9E1 (neutralizing Ab against P-selectin; R&D Systems) for 15 min, followed by the addition of rhsCD40L. After the treatments blood was processed and analyzed as described above for the detection of $CD14^+$ PMCs.

Platelet–monocyte co-culture

Monocytes were isolated from HIV-1–uninfected donors as described above and incubated overnight at 37°C. The next day, platelets were isolated from the same donor and treated with 1 μg/ml rhsCD40L, or were left untreated, for 20 min at 37°C. The platelets were washed with Tyrode's buffer and mixed with monocytes at a ratio of 10:1. Monocytes with or without rhsCD40L treatment were used as controls. Mixed cultures were incubated for 1 h at 37°C, following which half of the cells were fixed with 4% paraformaldehyde and stained with Abs against CD14, CD16, CD61, and CD62P. The remaining cells were incubated for 20 h and subsequently stained with Abs against PSGL-1-FITC, CCR2-FITC, or CD40-FITC in separate tubes. Five thousand monocytes were acquired on an Accuri C6 flow cytometer and were analyzed for detection of $CD14^+$ PMCs (after 1 h of mixed cultures) or various cell surface markers (after 20 h of mixed cultures).

Monocyte adhesion assay

This experiment was performed as described previously (27). Briefly, 2×10^4 BMVECs per well were plated onto black-walled, transparent-bottom 96-well plates (Corning, Corning, NY) that had been coated with rat-tail collagen type I (BD Biosciences). After the formation of confluent monolayers, the BMVECs were cultured without growth factors for 4–6 h and were then either treated with rhTNF-α (10 ng/ml; R&D Systems) to activate the endothelial cells or left untreated for 4 h. Monocytes and platelets were isolated separately from whole blood obtained from the same HIV-1–uninfected donor ($n = 3$). Monocytes were labeled with calcein AM green (5 μM/1 × 10^6 cells for 45 min; Invitrogen Life Technologies, Carlsbad, CA). A coculture of monocytes and platelets that had been activated by rhsCD40L (1 μg/ml) was established, as described above. Monocytes treated with or without rhsCD40L, as well as monocytes treated with LPS (10 ng/ml), were used as controls. Twenty-four hours after treatment, 2.5×10^4 monocytes per well were added onto the BMVECs and were allowed to adhere for 30 min at 37°C. The plates were subsequently washed three times with PBS to rinse away any unattached cells, and the relative fluorescence was measured on a Spectramax M3 fluorescence plate reader (Molecular Devices, Sunnyvale, CA). Relative fluorescence unit values obtained using only the monolayer of BMVECs were subtracted from all readings as background and results are represented as the fold difference between the number of monocytes that attached to BMVECs under the different experimental conditions and the number of nontreated monocytes that attached to the untreated endothelial cells.

Transendothelial migration assay

This assay was performed as described previously (27) with some modifications. BMVECs were plated on rat-tail collagen coated FluoroBlok-tinted tissue culture inserts (with 3-μm pores; BD Biosciences) at the density of 2.5×10^4 cells/insert. Platelet and monocyte cocultures were established as described before ($n = 3$). Platelets were activated using 1 μg/ml

rhsCD40L in the presence or absence of 5 μg/ml 9E1 (neutralizing Ab against P-selectin; R&D Systems) for 20 min. The monocytes were either left untreated or were treated with 1 μg/ml rhsCD40L or with 5 μg/ml 9E1. The monocytes were alternatively mixed with activated platelets with or without 9E1 at the ratio of 1:10. One hour after treatment, 5×10^5 monocytes/treatment were stained with Abs against CD14-PE, CD16-PE-Cy7, and CD61-Alexa Fluor 647 and were acquired on an Accuri C6 flow cytometer to enumerate the percentage of $CD14^+$ PMCs. Two hours after treatment as well as 24 h after treatment, 5×10^5 monocytes/treatment were added to the upper chamber of FluoroBlok inserts in the presence or absence of MCP-1 (30 ng/ml; R&D Systems) in the lower chamber; that is, the monocytes were allowed to migrate with or without a chemokine gradient. The migration was allowed to continue up to 7 h at 37°C. After 7 h, the cells in the lower chamber were collected and stained with Abs against CD14-PE and CD16-PE-Cy7, as described previously. After staining, the cells were resuspended in 250 μl 1× PBS. Twenty microliters per sample was acquired on an Accuri C6 flow cytometer at slow speed and at the same instrument settings for each experiment, and the number of $CD14^+$ monocytes/20 μl/sample was obtained. Final number of migrated cells was estimated by subtracting the number of $CD14^+$ monocytes that had migrated in absence of MCP-1 (passive migration) from the number of $CD14^+$ monocytes that had migrated in presence of MCP-1 (active migration). A fold change in monocyte migration was then calculated by dividing the final number of migrated monocytes per treatment by the final number of migrated cells in untreated monocytes.

PMC detection by immunohistochemical staining of human brain sections

Immunohistochemistry was performed on serial sections from postmortem paraffin-embedded brain tissue of cases obtain from the National NeuroAIDS Tissue Consortium (Washington, DC). The area under observation included the basal ganglia and cortical regions from three HIV-E cases and from two seronegative age-matched controls (cases 1– 3 and cases 8 and 10) (28). The immunofluorescence was performed using standard methodology. Briefly, serial sections (5 μm in thickness) were baked at 65°C for 20 min followed by deparaffinization and rehydration. The tissue was then subjected to Ag retrieval by incubating the sections at 100°C in 10 mM sodium citrate buffer (pH 6.0) for 20 min. To minimize autofluorescence, the sections were placed for ~8 hrs 38 cm apart from a fluorescent lamp using a 13-W compact fluorescent bulb. To block nonspecific Ab binding, the slides were incubated with 1% goat serum in 1× PBS and 0.1% Triton X-100 (Sigma-Aldrich). For immunolabeling, the following primary Abs were used: mAbs to human CD68 (diluted 1:300; Abcam) and polyclonal Abs to human CD61 (1:200; Cell Signaling Technology). Tissue sections were then rinsed, and secondary Abs, including donkey anti-mouse conjugated to Alexa Fluor 488 (diluted 1:500; Invitrogen) or donkey anti-rabbit conjugated to Alexa Fluor 594 (diluted 1:500; Invitrogen), were added for 1 h. The slides were mounted with ProLong antifade reagent containing DAPI (for detection of nucleus; Invitrogen). Images (at ×40 or ×100 objective magnification) were acquired using a CoolSNAP EZ CCD camera (Photometrics) coupled to a Nikon i80 Eclipse. Both the acquisition and pseudocolor conversion were performed using the NIS-Elements software from Nikon.

Statistical Analysis

GraphPad Prism (version 4, GraphPad Software, La Jolla, CA) was used to perform all statistical analyses. Unpaired *t* tests were used to compare data obtained from HIV-1–infected and uninfected samples. For multiple groups statistical significance was determined using one-way ANNOVA followed by Bonferroni's test. Pearson correlation test was used to correlate PMCs and platelet activation. A p value <0.05 was considered significant.

Results

HIV-1 infection leads to elevated levels of $CD16^+$ PMCs, despite cART

Previous studies of cardiovascular diseases have shown that complexes between activated platelets and monocytes are inflammatory in nature and induce monocyte maturation (reviewed in Ref. 17). Because HIV-1 infection is a chronic inflammatory disease and is known to cause platelet activation, we conducted a pilot study to assess the levels of PMCs in HIV-1–infected individuals (21). Because we found that there was a significant increase in PMCs in HIV-1–infected individuals, we recruited more participants. Whole blood samples obtained from HIV^+ ($n = 36$) and HIV^- ($n = 37$) individuals were stained and subsequently analyzed using flow cytometry. HIV-1–infected individuals showed significantly increased levels of $CD16^+$ PMCs as compared with HIV-1–uninfected individuals ($p = 0.013$, $R^2 = 0.08369$; Fig. 1A). In contrast, $CD16^-$ PMCs and platelet–granulocyte complexes did not differ between the two groups (Fig. 1B, 1C). Platelets obtained from HIV-1–infected donors appeared activated as compared with uninfected samples, and these platelets exhibited increased expression of CD62P (P-selectin) on their surface ($p = 0.036$; Fig. 1D). Consistently, the percentage of $CD62P^+$ platelets in both HIV^+ and HIV^- population demonstrated a positive correlation with the percentage of $CD16^+$ PMCs ($p = 0.008$, $R^2 = 0.0888$; Fig. 1E). We also observed a significant increase in the percentage of $CD16^+$ monocytes in HIV-1–infected individuals, which correlated positively with the $CD16^+$ PMCs, whereas there was no difference in $CD16^-$ monocytes (data not shown). Additional representative samples from HIV^+ ($n = 5$) and HIV^- ($n = 6$) individuals were also stained and analyzed using ImageStream (Amnis) and demonstrated a similar increase in $CD16^+$ PMCs (data not shown).

Morphological characteristics of PMCs

Corresponding images generated from the ImageStream analysis of the PMCs indicated the presence of two types of complexes: those with one or more platelets attached to the surface of the monocyte (type 1; Fig. 2A), and another in which the monocytes express CD61 internally or on its surface (type 2; Fig. 2B). In all samples (HIV^+ and HIV^-) the percentage of type 1 complexes was significantly higher than type 2 complexes ($p = 0.0008$; Fig. 2C), and the percentage of $CD16^+$ type 1 complexes was increased in HIV-1–infected individuals ($p < 0.05$; Fig. 2D) and that of type 2 complexes showed a similarly elevated trend toward an increase ($p = 0.07$, Fig. 2E). The type 1 complexes were primarily observed with one or two platelets per monocyte; however, several cells demonstrated more than two platelets that had attached (range of one to four). The average number of platelets attached did not differ significantly between HIV-1–infected and uninfected samples (Fig. 2F). Consistently, images obtained using scanning electron microscopy and transmission electron microscopy also indicated that there were one to three platelets per monocyte (Fig. 2G, 2H).

The presence of type 2 complexes is very intriguing, as there were no platelets physically attached to these monocytes. Monocyte may express some level of CD61 on their surface, as a subunit of the vitronectin receptor (VNR). The exact level of expression of this receptor on primary monocytes is not well understood. A study by Weerasinghe et al. (29) detected low levels of VNR on monocytes. Another report by Lefrenie et al. (30) demonstrated total absence of VNR in primary monocytes unless these cells were further cultured in the presence of M-CSF for 3–5 d. It is noteworthy that the monocytes in our experiments are unexposed to such external stimuli. Furthermore, our transmission electron microscopy images of the type 1 complexes illustrate that the platelet and monocyte membranes remain in close proximity when complexed (Fig. 2H), which may facilitate the transfer of platelet microparticles (which often expresses CD61) (31–33) to the monocyte. This seems to be a more plausible explanation for the presence of type 2 complexes, as we did not observe fusion between the membranes of the two cell types.

sCD40L induces PMC formation via the interaction of platelet P-selectin with monocyte PSGL-1

Previously we reported that HIV-1–infected individuals with cognitive impairment have increased levels of sCD40L in their plasma and cerebrospinal fluid as compared with infected individuals

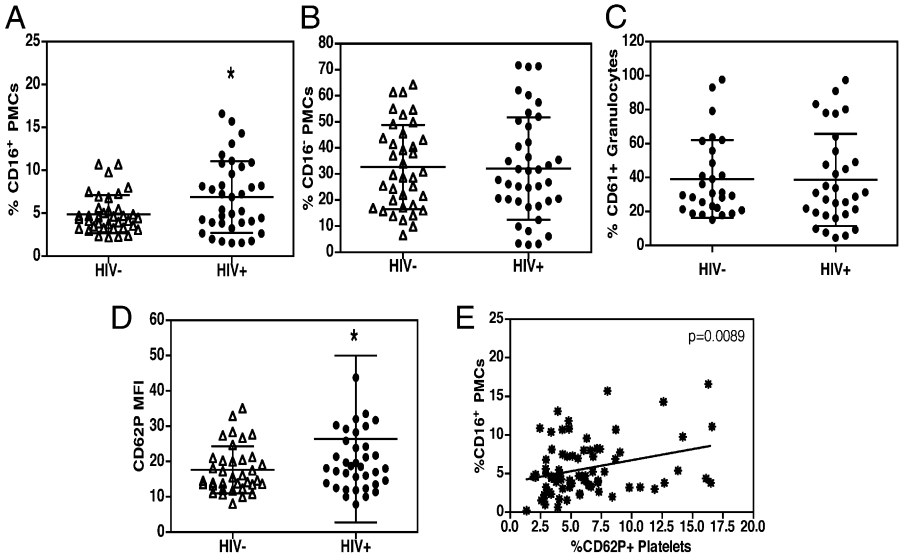

FIGURE 1. Detection of PMCs in HIV-1–infected and uninfected individuals. One hundred microliters whole blood obtained from HIV$^+$ (n = 36) and HIV$^-$ (n = 37) was fixed, stained with Abs against CD14, CD16, CD61, and CD62P (P-selectin), and subsequently acquired on an Accuri C6 flow cytometer. (**A**) CD16$^+$ PMCs were significantly increased in HIV-1–infected individuals. (**B**) There was no difference in CD16$^-$ PMCs between the two groups. (**C**) Platelet–granulocyte complexes did not differ between the groups. (**D**) Platelets from HIV-1–infected individuals expressed more CD62P (P-selectin) than platelets obtained from HIV$^-$ donors. (**E**) Platelet CD62P expression correlated positively with CD16$^+$ PMC percentages. In (A)–(D), samples were compared using an unpaired t test. *$p < 0.05$.

without cognitive impairment (24). To investigate the role of sCD40L in the platelet–monocyte interaction, wild-type C57BL/6J mice were injected with either saline or rmsCD40L (0.2 μg/g body weight), and PMC formation was subsequently analyzed in whole blood. CD40L-treated animals demonstrated a significant increase in total PMCs (p = 0.023, Fig. 3A), which was more pronounced in Gr-1^{hi} inflammatory complexes ($p < 0.0001$, Fig. 3B). As expected, sCD40L treatment induced a significant increase in platelet activation (p = 0.008, Fig. 3C) as compared with saline-treated animals.

In line with this, whole blood treatments using samples from HIV$^-$ donors also showed that treatment with rhsCD40L increases the degree of CD14$^+$ PMC formation (p = 0.006, Fig. 3D) and platelet activation ($p < 0.0001$, Fig. 3E) to levels comparable to ADP treatment (positive control, p = 0.006 for platelet activation and p = 0.0009 for PMCs). This effect was reduced by the addition of MK13, a neutralizing Ab raised against CD40L, indicating that the increase in PMCs was specifically due, in part, to CD40L. Similarly, 9E1, a blocking Ab raised against P-selectin, also ameliorated PMC formation, implying the involvement of the P-selectin–PSGL-1 interaction in PMC formation. Additionally, whereas MK13 treatment abrogated P-selectin (CD62P) expression by platelets, 9E1 had no effect on this marker (p = 0.001, Fig. 3D, 3E).

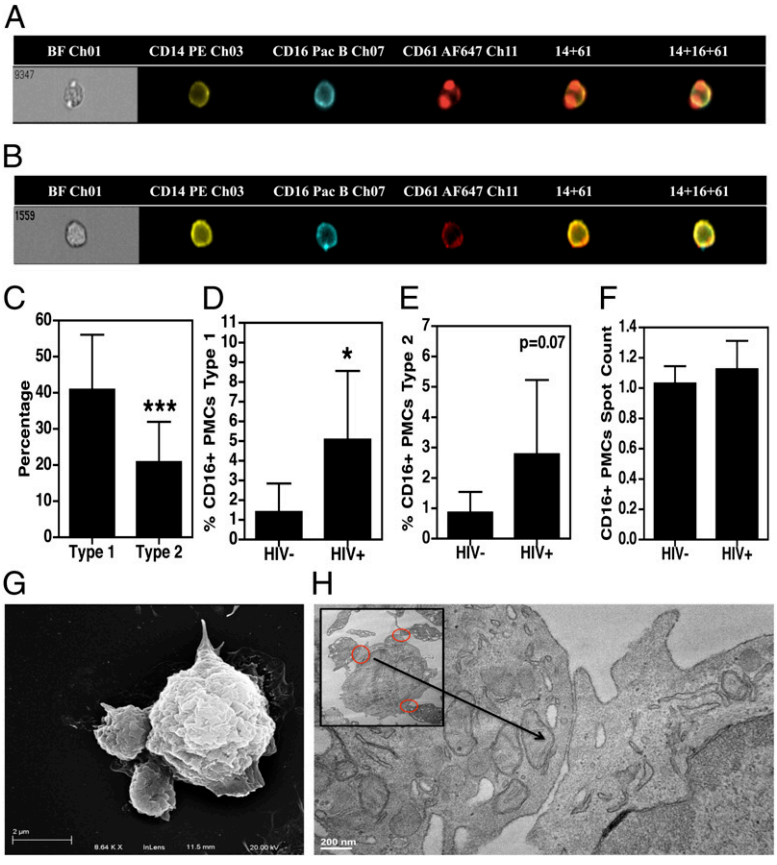

FIGURE 2. Morphological characterization of PMCs. (**A**–**F**) One hundred microliters whole blood obtained from HIV$^+$ (n = 5) and HIV$^-$ (n = 6) donors was fixed, stained with Abs against CD14, CD16, and CD61, and acquired on an Amnis ImageStream flow cytometer. (A and B) Representative images of type 1 and type 2 CD16$^+$ PMCs, respectively. Original magnification ×40. (C) Type 1 complexes were more prevalent in HIV-1–infected and uninfected samples. (D and E) HIV-1–infected individuals contain significantly higher percentages of type 1 and type 2 PMCs. (F) The average number of platelets per monocyte in a PMC did not differ between the two study groups. (**G** and **H**) Monocytes were isolated from PBMCs derived from HIV-1–seronegative subjects (n = 3) and were allowed to adhere to the culture dishes for 2 h. Cells were further processed for scanning electron microscopy (G) and transmission electron microscopy (H). (G and H) Original magnification ×800 [*inset* in (H) ×6000]. The red circles in (H) indicate platelets interacting with the monocyte. In (A)–(F), samples were compared using an unpaired t test. *$p < 0.05$, ***$p < 0.001$.

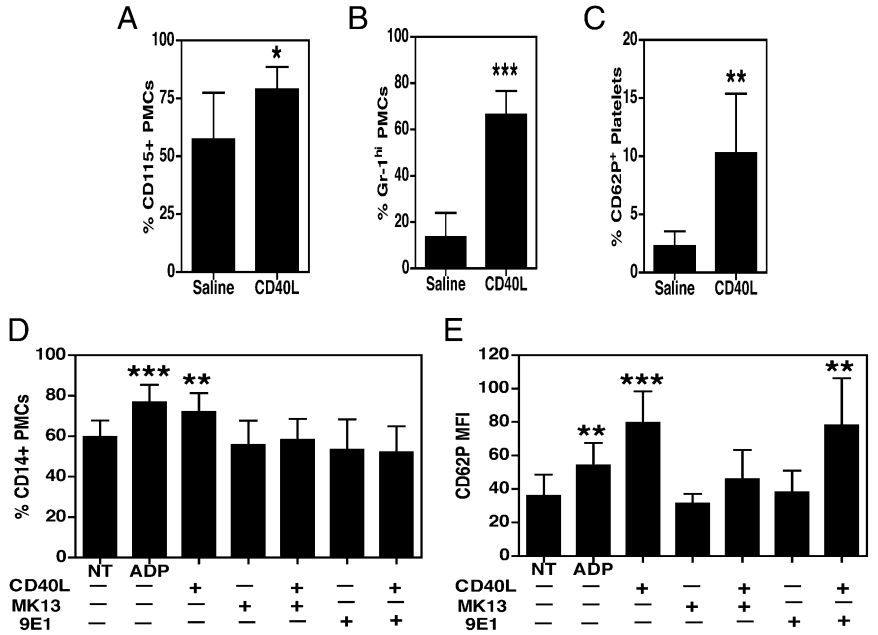

FIGURE 3. CD40L-induced platelet activation leads to PMC formation. (**A**–**C**) C57BL/6J mice were injected retro-orbitally with either rmsCD40L or saline ($n = 6$). Two hours after injection, blood was drawn, stained with Abs against CD115, Gr-1, CD61, and CD62P (P-selectin), and acquired on an Accuri C6 flow cytometer. (A and B) Injection of rmsCD40L lead to a significant increase in PMCs, with a more pronounced difference in the inflammatory Gr-1^{hi} monocyte subset. (C) rmsCD40L also caused an increase in platelet CD62P expression. (**D** and **E**) Whole blood obtained from HIV$^-$ study participants ($n = 4$) was treated with ADP or rhsCD40L in the presence or absence of either MK13 (neutralizing Ab against CD40L) or 9E1 (a blocking Ab against P-selectin). The blood was then processed as described previously for the detection of PMCs using an Accuri C6 flow cytometer. (D) CD40L induced a significant increase in percentage for CD14$^+$ PMCs, which was abrogated by both MK13 and 9E1. (E) CD40L treatment leads to an increase in CD62P (P-selectin) expression on platelets, which was reversed by MK13 but not by 9E1. Samples in (A)–(C) were compared using an unpaired t test, and samples in (D) and (E) were compared using one-way ANNOVA followed by Bonferroni's test. $^*p < 0.05$, $^{**}p < 0.01$, $^{***}p < 0.001$.

Monocytes in complex with activated platelets exhibit an enhanced proinflammatory and promigratory phenotype

To further investigate the effect of the interaction of monocytes with platelets on monocyte activation, we developed a coculture system using platelets and monocytes isolated from HIV-1–ninfected donors. Platelets were either treated using rhsCD40L, or left untreated, and analyzed for P-selectin (CD62P) expression to verify activation status (Fig. 4A). The platelets were subsequently mixed with monocytes, and the cocultures were then used for the detection of CD14$^+$ PMCs, as well as analysis of cell surface expression of CCR2, PSGL-1, and CD40 on the complexed monocytes. Single-cell type cultures were also treated in parallel and used as controls. Platelets that were pretreated with rhsCD40L induced significantly higher levels of PMC formation upon mixture with monocytes, as compared with platelets that had been left untreated ($p = 0.029$, Fig. 4B). This effect of platelets on PMC formation was not due to direct action of rhsCD40L on monocytes because such treatment failed to increase CD16 expression on monocytes (data not shown). Monocytes in complex with activated platelets showed elevated expression of CCR2 ($p = 0.07$, Fig. 4C), PSGL-1 ($p = 0.048$, Fig. 4D), and CD40 ($p = 0.017$, Fig. 4E). Additionally, in some experiments, the platelet–monocyte cocultures were allowed to adhere to BMVECs that were either nonactivated or were activated using TNF-α for 30 min. Monocytes that had been cocultured with activated platelets demonstrated enhanced adhesion to endothelial cells, regardless of endothelial cell activation status ($p < 0.01$, Fig. 5A).

Interaction of monocytes with activated platelets promotes transendothelial migration of monocytes

Because monocytes in complex with activated platelets showed increased adherence to BMVECs, we sought to investigate whether these cells also migrate more efficiently through the transendothelial barrier. We established platelet–monocyte cocultures as described previously. Additionally, this time we used 9E1, which is a P-selectin blocking Ab, to prevent P-selectin–dependent formation of PMCs. One hour after treatment, cells were stained and acquired to enumerate the percentages of CD14$^+$ PMCs. Consistent with the data shown in Fig. 3D, coculturing of rhsCD40L-exposed platelets with monocytes resulted in significantly higher levels of PMC formation ($p < 0.001$ as compared with untreated monocytes), whereas activated platelets that were treated with 9E1 showed significantly reduced PMC formation ($p < 0.05$ as compared with monocytes treated with activated platelets, data not shown). Twenty-four hours later the cells were allowed to migrate through a monolayer of BMVECs. It was our speculation that the incubation of PMCs for 24 h will lead to enhanced expression of CCR2, PSGL-1, and CD40, followed by increased adhesion to BMVECs (as shown in Figs. 4C–E, 5A). As expected, higher numbers of CD14$^+$ monocytes that were treated with activated platelets migrated through the BMVEC monolayer ($p < 0.01$ as compared with untreated monocytes). Interestingly, this population of monocytes appeared to be predominantly CD16$^+$ (>65%; data not shown). Alternatively, the migration of monocytes was significantly reduced when PMC formation was blocked with the use of 9E1 Ab ($p < 0.05$ as compared with monocytes treated with activated platelets, Fig. 5B).

Immunohistochemical evidence of PMCs in brain tissue from cases of HIV-E

We next sought to evaluate whether PMCs could be detected in the CNS of individuals that had prominent neuropathology due to HIV-1 infection. Postmortem tissues derived from basal ganglia and the cortical region of three patients with HIV-E and two

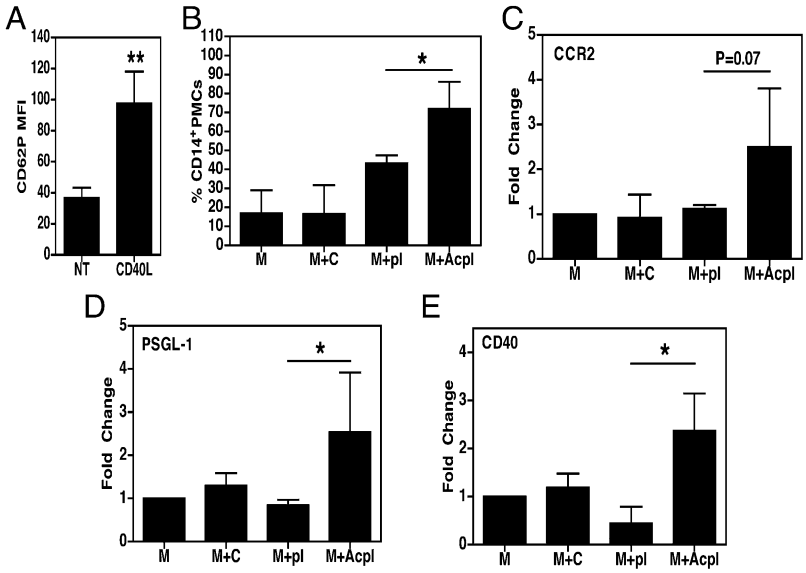

FIGURE 4. Interaction with activated platelets increases the expression of functionally important molecules on monocytes. Monocytes and platelets were isolated separately from whole blood obtained from HIV$^-$ donors ($n = 4$). Platelets were either treated with rhsCD40L or were left untreated, and were subsequently mixed with monocytes at the ratio of 10:1. M indicates nontreated monocytes, M+C indicates monocytes treated with CD40L, M+pl indicates monocytes treated with nonactivated platelets, and M+Acpl indicates monocytes treated with CD40L-activated platelets. (**A** and **B**) One hour after coculture, cells were used to enumerate PMCs as described before. Platelets activated using rhsCD40L led to an increase in percentage of CD14+ PMCs as compared with unactivated platelets. (**C**–**E**) Twenty hours after coculture, monocytes were stained with Abs against CCR2, CD40, and PSGL-1 in addition to Abs for the detection of PMCs. There was a significant increase in the percentage of monocytes expressing of CCR2, CD40, and PSGL-1 upon interaction with activated platelets as compared with monocytes in complex with unactivated platelets. Samples in (A) were compared using an unpaired *t* test, and samples in (B)–(E) were compared using one-way ANNOVA followed by Bonferroni's test. $*p < 0.05$, $**p < 0.01$.

HIV-1–seronegative patients were double immunolabeled for CD68 (monocyte/macrophage marker) and CD61. Clinical, pathologic, and demographic details of these cases have been published before (28, 34). As shown in Fig. 6, the brain specimens obtained from patients with HIV-E contained evidence of PMCs, both in the lumen (Fig. 6C, 6D, 6F; only basal ganglia regions are shown) and marginalized (attached to the endothelium) to the brain microvasculature (Fig. 6E, 6F). Of note, there was an increased presence of type 1 PMCs featuring multiple platelets on a single monocyte/macrophage (Fig. 6C–G). In contrast, no PMCs were observed in control brain samples derived from HIV-1–seronegative subjects (Fig. 6A, 6B). Although CD68$^+$ cells in the perivascular space were seen in perivascular cuffs and disseminated throughout the brain parenchyma, no platelets were detected alone or in complex with monocytes within the perivascular space or in the parenchyma. As previously noted, these tissues have extensive neuroinflammation, showing microgliosis (as revealed by Iba-1 Abs) and infiltrating CD68$^+$ cells that are also immunoreactive for the HIV-1 p24 core Ag (34). These results suggest that the increased presence of PMCs is associated with HIV-1–induced neuroinflammation, thus offering the possibility that PMCs contribute to immune cell migration and breach of the BBB during infection.

Discussion

HIV-1–associated neuroinflammation and HIV-E are associated with excess immune activation, which outweighs the amount of virus present within the CNS (7). The inflammatory response from resident, as well as infiltrating, monocytes and macrophages is known to fuel the neuropathogenesis of these disorders (12). To transmigrate into the CNS, monocytes must traverse the BBB, formed by endothelial cells that line the cerebral vasculature. Immune transendothelial migration can alter the normal function of the neurovascular unit, which consists of endothelial cells, astrocytes, pericytes, and neurons. We have previously indicated that sCD40L secreted by aberrantly activated platelets is implicated in the impairment of the BBB during HIV-1 infection (26), thereby providing monocytes with an increased chance of thwarting this barrier. Furthermore, almost all cells of the monocytic lineage found within the CNS of HIV-1–infected individuals are CD16$^+$ proinflammatory monocytes (12). Importantly, CD16$^+$ monocytes are well known for their invasiveness across endothelial barriers. Interestingly, the findings in the present study now serve to bridge these reports, wherein we demonstrate that during HIV-1 infection, activated platelets interact more frequently with monocytes that consequently promote a proinflammatory and promigratory phenotype and cause an increase in the migration of these monocytes across the transendothelial barrier. Thus, these monocytes, with an enhanced capacity to transmigrate, are better equipped to extravasate through a compromised BBB and, consequently, contribute to neuroinflammation.

Consistent with this notion, we now demonstrate that HIV-1–infected individuals enrolled in our study showed the occurrence of increased circulating PMCs, especially in the CD16$^+$ inflammatory monocyte subset, as well as increased platelet activation, despite successful cART. Studies have shown an increased incidence of milder forms of HAND in patients treated with cART (35). Thus, these studies highlight the need for the development of adjunctive therapies to supplement cART that could limit the neurologic complications associated with infection. The data reported in the present study, as well as previous studies from our group, indicate that modulation of platelet activation, and more specifically the release of sCD40L, may be a novel therapeutic target for these disorders. We previously demonstrated that the formation of PMCs was an event subsequent to platelet activation, and not monocyte activation (21), whereas we now report that PMCs have an enhanced migratory and invasive phenotype.

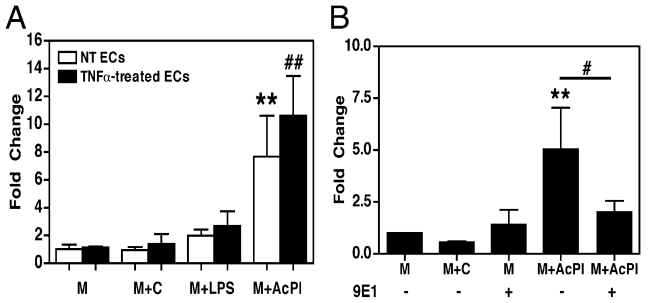

FIGURE 5. Monocytes in PMCs display increased adherence to endothelium and enhanced transendothelial migration. (**A**) Monocytes isolated from HIV-1–uninfected blood samples ($n = 3$) were labeled with calcein AM green and were either cocultured with activated platelets or, alternatively, treated with rhsCD40L, LPS, or left untreated. Twenty-four hours after treatment cells were allowed to adhere to BMVECs that had been treated with TNF-α or that were left untreated. Fluorescence from adhered cells was measured using a fluorescent plate reader. Results are represented as the fold difference between the number of monocytes that attached to BMVECs under the different experimental conditions and the number of nontreated monocytes that attached to the untreated endothelial cells. Monocytes in complex with activated platelets showed increased adherence to BMVECs. Samples were compared using one-way ANNOVA followed by Bonferroni's test: $^{**}p < 0.01$, $^{\#\#}p < 0.01$ as compared with nontreated monocytes that adhered to nonactivated and activated BMVECs, respectively. (**B**) Monocytes isolated from HIV-1–uninfected blood samples ($n = 3$) were either cocultured with platelets activated using rhsCD40L in the presence or absence of 9E1, a P-selectin blocking Ab, or, alternatively, treated with rhsCD40L, 9E1, or left untreated. One hour after treatment the cells were used to detect PMCs and 24 h after treatment the cells were allowed to migrate across the BMVEC monolayer plated on FluoroBlok tissue culture inserts with 3 μm pore size, and the number of migrated $CD14^+$ monocytes was calculated for each treatment. Results of the migration experiment are represented as the fold difference between the numbers of migrated $CD14^+$ monocytes among various treatments and untreated monocytes. M indicates nontreated monocytes, M+C indicates monocytes treated with CD40L, M+9E1 indicates monocytes treated with 9E1 Ab, M+ Acpl indicates monocytes treated with CD40L-activated platelets, and M+AcPl+9E1 indicates monocytes mixed with platelets that were activated with CD40L in the presence of 9E1 Ab. Monocytes in complex with activated platelets showed significantly increased migration across BMVECs as compared with untreated monocytes as well as cultures where PMC formation was blocked through use of 9E1 Ab. Samples were compared using one-way ANNOVA followed by Bonferroni's test. $^{**}p < 0.01$ as compared with untreated monocytes, and $^{\#}p < 0.05$ as compared with monocytes that were treated with platelets activated in the presence of 9E1 Ab.

sCD40L is almost entirely platelet derived (25, 26), and in the present study, the role of CD40L signaling in the generation of PMCs was corroborated via in vitro coculture of monocytes with CD40L-activated or nonactivated platelets. These experiments demonstrated that monocytes in complex with CD40L-activated platelets express higher levels of CCR2, a chemokine receptor important for MCP-1–driven chemotaxis of monocytes into the CNS. PSGL-1, which is necessary for the interaction of monocytes with not only platelets, but also with endothelial cells, and CD40, which is a costimulatory molecule and the receptor for CD40L, were also elevated in monocytes incubated with CD40L-activated platelets. Monocytes that were exposed to CD40L-activated platelets also demonstrated an increased propensity to adhere to endothelial cells and migrate across the BMVEC monolayer as compared with nonactivated monocytes. Corroborating the in vitro results, immunohistochemical analysis of brain tissue samples from patients with HIV-E showed an increased presence of PMCs lining the brain endothelium (lumen) within the basal ganglia and cortical regions, as compared with tissue from uninfected controls.

These data are consistent with the notion that excess levels of sCD40L, and thus platelet activation, found in the plasma of HIV-1 patients (24, 26, 36, 37) contributes to the pathogenesis of neurologic disorders presumably via formation of PMCs, leading to invasion of the CNS by activated monocytes/macrophages. Indeed, our recent report also highlighted the ability of BMVECs to respond to CD40L in a manner that promotes monocyte attachment and migration, as exposure of primary human BMVECs to sCD40L in vitro leads to increased expression of adhesion molecules, ICAM-1 and VCAM-1. The same study also showed that the receptor for CD40L, CD40, was found to be highly expressed on endothelial cells in brain tissue collected from HIV-E patients (28). Consistently, other studies speculated that the interaction between platelets and monocytes increases the expression and activity of $\alpha_4\beta_1$ and $\alpha_M\beta_2$ integrins on monocytes (15, 38), thereby exhibiting increased ability of primary and secondary tethering to endothelial cells and other inflammatory cells (39, 40).

Interestingly, short-term treatment with low-dose aspirin, a known antiplatelet agent, was able to attenuate platelet and immune activation in virologically suppressed HIV-1–infected individuals (41). Furthermore, Gremmel et al. (42) have shown that prasugrel, an ADP receptor antagonist, reduces agonist-induced platelet activation and platelet–leukocyte interactions. Similarly, the clinically used mood stabilizer valproic acid exerts antiplatelet activity in a manner that attenuates sCD40L levels in HIV-1–infected individuals (36). It is noteworthy that the valproic acid treatment improves cognitive performance, as well as indices of brain metabolism, when tested in a controlled pilot study of HIV-1–infected individuals (43). Thus, dampening platelet activation, and in turn PMC formation, with antiplatelet agents such as aspirin, prasugrel, or valproic acid may prove a worthy avenue of pursuit in developing adjunctive therapies for use in combination with cART in an effort to reduce HIV-1–associated inflammatory illnesses such as HAND and cardiovascular disease. Indeed, PMCs are a known risk factor for cardiovascular disease, and HIV-1–infected individuals are at an increased risk for developing these secondary disorders (44, 45). Therefore, the use of antiplatelet agents as an adjunctive therapeutic strategy for HIV-1 infection may have benefits that are multifactorial.

Formation of PMCs appears to be a very rapid phenomenon, as injection of rmsCD40L caused an increase in total ($CD115^+$) as well as Gr-1^{hi} (inflammatory murine monocyte subset) PMCs in mice as early as 2 h posttreatment. Gr-1^{hi} monocytes are the functional counterpart in mice for $CD16^+$ monocytes in human, as these cells initiate inflammatory activity and accumulate at the sites of injury more abundantly than do Gr-1^{lo} monocytes (46). Consistently, ex vivo treatments using rhsCD40L in whole blood samples obtained from HIV-1–seronegative individuals also induced the formation of PMCs within 1 h, an effect that was nullified by the use of a neutralizing Ab raised against CD40L (MK13). Blockade of P-selectin on platelets using the blocking Ab 9E1 did not affect platelet activation in response to rhsCD40L, but it significantly inhibited PMC formation, indicating the involvement of P-selectin–PSGL-1 interaction during PMC formation. Additional molecules known to be involved in platelet–monocyte interactions include EMMPRIN (47), CX3CR1 (48), and monocytic CD115 with platelet P-selectin. However, the association of PSGL-1 with platelet P-selectin is considered to be the most critical interface, whereas other ligands play an additive role (17). Collectively, these results indicate that inhibition of sCD40L signaling with antiplatelet agents would be capable of attenuating the formation of PMCs, further highlighting the potential benefits of

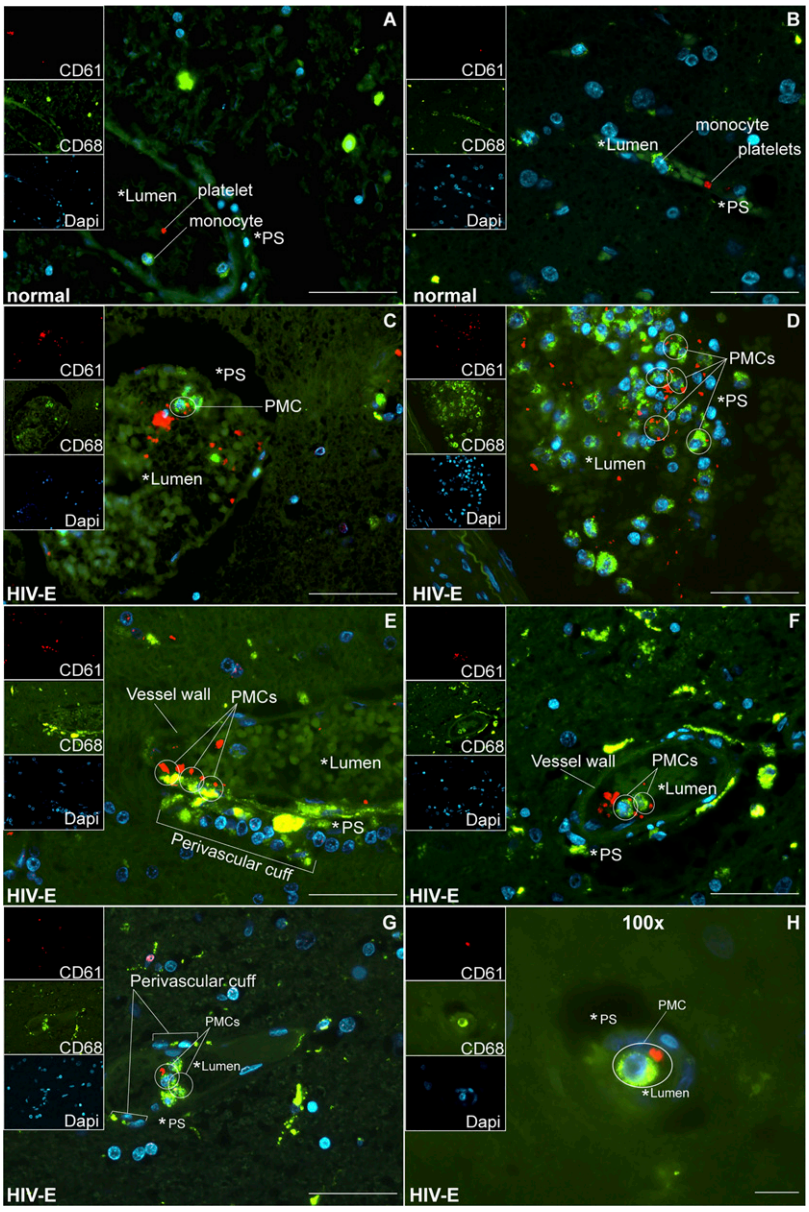

FIGURE 6. Immunohistochemical analysis showed PMCs marginalized to the endothelial wall in brain tissue samples obtained from individuals with HIV-E. Postmortem brain tissue sections from HIV-1–seronegative individuals ($n = 2$) (**A**, **B**) and individuals with HIV-E ($n = 3$) (**C**–**H**) were immunostained using indirect immunofluorescence with Abs against CD68 (monocytic marker, green) and CD61 (platelet marker, red). Sections were also counterstained with DAPI (blue) to aid in the identification of nucleated cells and platelet clusters. (A) and (B) show tissue sections from uninfected controls lacking PMCs, which only display uncoupled $CD61^+$ platelets and $CD68^+$ monocytes. (C), (D), and (F) exemplify traveling PMCs present in vessel lumens of HIV-E cases. (E) and (G) indicate PMCs appearing as lined or marginalized to the endothelial wall in areas where perivascular cuffing was also evident. (H) shows a high magnification image of a traveling PMC inside a cerebral capillary vessel. An asterisk denotes the perivascular space (PS) and vessel lumens in relationship to the brain parenchyma. Images were taken at either ×40 or ×100 (objective magnifications). Scale bars are 50 μm and 10 μm for the ×40 and ×100 objective magnifications, respectively.

antiplatelet therapies for the management of neuroinflammatory consequences of HIV-1 infection in patients.

Presence of $CD68^+$ monocytes/macrophages in the perivascular space and adjoining parenchymal regions within HIV-E brain is clearly evident; however, we were unable to detect PMCs and/or platelets that had extravasated into the brain of these patients. Platelets are occasionally shown to possess the ability to extravasate into tissues. For example, a study by Laidlaw et al. (49) reported the presence of platelet–leukocyte complexes in inflamed respiratory tissue of subjects with aspirin-exacerbated respiratory disease, whereas another report by Pitchford et al. (50) indicated that platelets migrate extravascularly in response to a sensitizing allergen and can participate directly in allergic tissue inflammation in a mouse model. In contrast to these observations, a recent report by van Gils et al. (51) suggested that platelets relocate with monocytic PSGL-1 to the rear of the monocyte, following adherence to the endothelium, subsequently detach from monocytes, and remain at the endothelial cell surface. Our data are consistent with those of van Gils et al. and suggest that the platelets may not leave the circulation; however, association with activated platelets in the periphery could prime monocytes to migrate into the CNS, with the release of the platelet behind in the vessel lumen.

Taken together, our findings substantiate the role of PMCs in HIV-1–associated neuroinflammation. In the post-cART era, the severity of neurologic diseases has been reduced; however, with the increased lifespan of HIV-1–infected individuals, mild and asymptomatic forms of neurocognitive impairment are increasing in prevalence (reviewed in Ref. 35). Although this means that the morbidity associated with neurologic complications has been lessened, milder forms of the disease can still interfere with the day-to-day functions of an individual, and can often be predictive of more severe forms of these disorders. Given the current absence of effective therapeutic options to address this aspect of the disease, the results presented in this study shed light on the underlying mechanisms that may drive the pathogenesis of HIV-1–associated neuroinflammation, thereby identifying novel targets for the development of adjunctive therapies and highlighting the potential utility of antiplatelet agents as such.

Acknowledgments

We thank the University of Rochester Infectious Disease Unit and the Rochester Victory Alliance (Rochester, NY), specifically Carol Greisberger,

Catherine Bunce, Emily Cosimano, Mary Adams, Chris Foote, and Ann Casey for help in recruiting study subjects. We thank Karen Bentley at the University of Rochester Electron Microscopy Core, as well as Linda Callahan, Maria Jepson, and Paivi Jordan at the University of Rochester Multiphoton Core.

Disclosures

The authors have no financial conflicts of interest.

References

1. Davis, L. E., B. L. Hjelle, V. E. Miller, D. L. Palmer, A. L. Llewellyn, T. L. Merlin, S. A. Young, R. G. Mills, W. Wachsman, and C. A. Wiley. 1992. Early viral brain invasion in iatrogenic human immunodeficiency virus infection. *Neurology* 42: 1736–1739.
2. Alexaki, A., Y. Liu, and B. Wigdahl. 2008. Cellular reservoirs of HIV-1 and their role in viral persistence. *Curr. HIV Res.* 6: 388–400.
3. Petito, C. K., E. S. Cho, W. Lemann, B. A. Navia, and R. W. Price. 1986. Neuropathology of acquired immunodeficiency syndrome (AIDS): an autopsy review. *J. Neuropathol. Exp. Neurol.* 45: 635–646.
4. Heaton, R. K., D. B. Clifford, D. R. Franklin, Jr., S. P. Woods, C. Ake, F. Vaida, R. J. Ellis, S. L. Letendre, T. D. Marcotte, J. H. Atkinson, et al; CHARTER Group. 2010. HIV-associated neurocognitive disorders persist in the era of potent antiretroviral therapy: CHARTER Study. *Neurology* 75: 2087–2096.
5. Bezzi, P., M. Domercq, L. Brambilla, R. Galli, D. Schols, E. De Clercq, A. Vescovi, G. Bagetta, G. Kollias, J. Meldolesi, and A. Volterra. 2001. CXCR4-activated astrocyte glutamate release via TNFα: amplification by microglia triggers neurotoxicity. *Nat. Neurosci.* 4: 702–710.
6. Kaul, M., and S. A. Lipton. 1999. Chemokines and activated macrophages in HIV gp120-induced neuronal apoptosis. *Proc. Natl. Acad. Sci. USA* 96: 8212–8216.
7. Glass, J. D., H. Fedor, S. L. Wesselingh, and J. C. McArthur. 1995. Immunocytochemical quantitation of human immunodeficiency virus in the brain: correlations with dementia. *Ann. Neurol.* 38: 755–762.
8. Kaul, M., J. Zheng, S. Okamoto, H. E. Gendelman, and S. A. Lipton. 2005. HIV-1 infection and AIDS: consequences for the central nervous system. *Cell Death Differ.* 12(Suppl. 1): 878–892.
9. Strauss-Ayali, D., S. M. Conrad, and D. M. Mosser. 2007. Monocyte subpopulations and their differentiation patterns during infection. *J. Leukoc. Biol.* 82: 244–252.
10. Thieblemont, N., L. Weiss, H. M. Sadeghi, C. Estcourt, and N. Haeffner-Cavaillon. 1995. $CD14^{low}CD16^{high}$: a cytokine-producing monocyte subset which expands during human immunodeficiency virus infection. *Eur. J. Immunol.* 25: 3418–3424.
11. Ellery, P. J., E. Tippett, Y. L. Chiu, G. Paukovics, P. U. Cameron, A. Solomon, S. R. Lewin, P. R. Gorry, A. Jaworowski, W. C. Greene, et al. 2007. The $CD16^+$ monocyte subset is more permissive to infection and preferentially harbors HIV-1 in vivo. *J. Immunol.* 178: 6581–6589.
12. Fischer-Smith, T., C. Bell, S. Croul, M. Lewis, and J. Rappaport. 2008. Monocyte/macrophage trafficking in acquired immunodeficiency syndrome encephalitis: lessons from human and nonhuman primate studies. *J. Neurovirol.* 14: 318–326.
13. Fischer-Smith, T., S. Croul, A. E. Sverstiuk, C. Capini, D. L'Heureux, E. G. Régulier, M. W. Richardson, S. Amini, S. Morgello, K. Khalili, and J. Rappaport. 2001. CNS invasion by $CD14^+/CD16^+$ peripheral blood-derived monocytes in HIV dementia: perivascular accumulation and reservoir of HIV infection. *J. Neurovirol.* 7: 528–541.
14. Pulliam, L., R. Gascon, M. Stubblebine, D. McGuire, and M. S. McGrath. 1997. Unique monocyte subset in patients with AIDS dementia. *Lancet* 349: 692–695.
15. da Costa Martins, P. A., J. M. van Gils, A. Mol, P. L. Hordijk, and J. J. Zwaginga. 2006. Platelet binding to monocytes increases the adhesive properties of monocytes by up-regulating the expression and functionality of β_1 and β_2 integrins. *J. Leukoc. Biol.* 79: 499–507.
16. Ancuta, P., R. Rao, A. Moses, A. Mehle, S. K. Shaw, F. W. Luscinskas, and D. Gabuzda. 2003. Fractalkine preferentially mediates arrest and migration of $CD16^+$ monocytes. *J. Exp. Med.* 197: 1701–1707.
17. van Gils, J. M., J. J. Zwaginga, and P. L. Hordijk. 2009. Molecular and functional interactions among monocytes, platelets, and endothelial cells and their relevance for cardiovascular diseases. *J. Leukoc. Biol.* 85: 195–204.
18. Elalamy, I., T. Chakroun, G. T. Gerotziafas, A. Petropoulou, F. Robert, A. Karroum, F. Elgrably, M. M. Samama, and M. Hatmi. 2008. Circulating platelet-leukocyte aggregates: a marker of microvascular injury in diabetic patients. *Thromb. Res.* 121: 843–848.
19. Furman, M. I., M. R. Barnard, L. A. Krueger, M. L. Fox, E. A. Shilale, D. M. Lessard, P. Marchese, A. L. Frelinger, III, R. J. Goldberg, and A. D. Michelson. 2001. Circulating monocyte-platelet aggregates are an early marker of acute myocardial infarction. *J. Am. Coll. Cardiol.* 38: 1002–1006.
20. Rinder, H. M., J. L. Bonan, C. S. Rinder, K. A. Ault, and B. R. Smith. 1991. Dynamics of leukocyte-platelet adhesion in whole blood. *Blood* 78: 1730–1737.
21. Singh, M. V., D. C. Davidson, M. Kiebala, and S. B. Maggirwar. 2012. Detection of circulating platelet-monocyte complexes in persons infected with human immunodeficiency virus type-1. *J. Virol. Methods* 181: 170–176.
22. Li, N., H. Hu, M. Lindqvist, E. Wikström-Jonsson, A. H. Goodall, and P. Hjemdahl. 2000. Platelet-leukocyte cross talk in whole blood. *Arterioscler. Thromb. Vasc. Biol.* 20: 2702–2708.
23. Holme, P. A., F. Müller, N. O. Solum, F. Brosstad, S. S. Frøland, and P. Aukrust. 1998. Enhanced activation of platelets with abnormal release of RANTES in human immunodeficiency virus type 1 infection. *FASEB J.* 12: 79–89.
24. Sui, Z., L. F. Sniderhan, G. Schifitto, R. P. Phipps, H. A. Gelbard, S. Dewhurst, and S. B. Maggirwar. 2007. Functional synergy between CD40 ligand and HIV-1 Tat contributes to inflammation: implications in HIV type 1 dementia. *J. Immunol.* 178: 3226–3236.
25. André, P., L. Nannizzi-Alaimo, S. K. Prasad, and D. R. Phillips. 2002. Platelet-derived CD40L: the switch-hitting player of cardiovascular disease. *Circulation* 106: 896–899.
26. Davidson, D. C., M. P. Hirschman, A. Sun, M. V. Singh, K. Kasischke, and S. B. Maggirwar. 2012. Excess soluble CD40L contributes to blood brain barrier permeability in vivo: implications for HIV-associated neurocognitive disorders. *PLoS ONE* 7: e51793.
27. Ramirez, S. H., D. Heilman, B. Morsey, R. Potula, J. Haorah, and Y. Persidsky. 2008. Activation of peroxisome proliferator-activated receptor γ (PPARγ) suppresses Rho GTPases in human brain microvascular endothelial cells and inhibits adhesion and transendothelial migration of HIV-1 infected monocytes. *J. Immunol.* 180: 1854–1865.
28. Ramirez, S. H., S. Fan, H. Dykstra, N. Reichenbach, L. Del Valle, R. Potula, R. P. Phipps, S. B. Maggirwar, and Y. Persidsky. 2010. Dyad of CD40/CD40 ligand fosters neuroinflammation at the blood-brain barrier and is regulated via JNK signaling: implications for HIV-1 encephalitis. *J. Neurosci.* 30: 9454–9464.
29. Weerasinghe, D., K. P. McHugh, F. P. Ross, E. J. Brown, R. H. Gisler, and B. A. Imhof. 1998. A role for the $\alpha_v\beta_3$ integrin in the transmigration of monocytes. *J. Cell Biol.* 142: 595–607.
30. Lafrenie, R. M., S. F. Lee, I. K. Hewlett, K. M. Yamada, and S. Dhawan. 2002. Involvement of integrin $\alpha_v\beta_3$ in the pathogenesis of human immunodeficiency virus type 1 infection in monocytes. *Virology* 297: 31–38.
31. Rank, A., R. Nieuwland, R. Delker, V. Pihusch, R. Wilkowski, B. Toth, H. J. Kolb, and R. Pihusch. 2011. Surveillance of megakaryocytic function by measurement of CD61-exposing microparticles in allogeneic hematopoietic stem cell recipients. *Clin. Transplant.* 25: E233–E242.
32. George, J. N., L. L. Thoi, L. M. McManus, and T. A. Reimann. 1982. Isolation of human platelet membrane microparticles from plasma and serum. *Blood* 60: 834–840.
33. Heijnen, H. F., A. E. Schiel, R. Fijnheer, H. J. Geuze, and J. J. Sixma. 1999. Activated platelets release two types of membrane vesicles: microvesicles by surface shedding and exosomes derived from exocytosis of multivesicular bodies and α-granules. *Blood* 94: 3791–3799.
34. Ramirez, S. H., N. L. Reichenbach, S. Fan, S. Rom, S. F. Merkel, X. Wang, W. Z. Ho, and Y. Persidsky. 2013. Attenuation of HIV-1 replication in macrophages by cannabinoid receptor 2 agonists. *J. Leukoc. Biol.* 93: 801–810.
35. McArthur, J. C., J. Steiner, N. Sacktor, and A. Nath. 2010. Human immunodeficiency virus-associated neurocognitive disorders: mind the gap. *Ann. Neurol.* 67: 699–714.
36. Davidson, D. C., M. P. Hirschman, S. L. Spinelli, C. N. Morrell, G. Schifitto, R. P. Phipps, and S. B. Maggirwar. 2011. Antiplatelet activity of valproic acid contributes to decreased soluble CD40 ligand production in HIV type 1-infected individuals. *J. Immunol.* 186: 584–591.
37. Davidson, D. C., G. Schifitto, and S. B. Maggirwar. 2013. Valproic acid inhibits the release of soluble CD40L induced by non-nucleoside reverse transcriptase inhibitors in human immunodeficiency virus infected individuals. *PLoS ONE* 8: e59950.
38. Yago, T., M. Tsukuda, and M. Minami. 1999. P-selectin binding promotes the adhesion of monocytes to VCAM-1 under flow conditions. *J. Immunol.* 163: 367–373.
39. da Costa Martins, P., N. van den Berk, L. H. Ulfman, L. Koenderman, P. L. Hordijk, and J. J. Zwaginga. 2004. Platelet-monocyte complexes support monocyte adhesion to endothelium by enhancing secondary tethering and cluster formation. *Arterioscler. Thromb. Vasc. Biol.* 24: 193–199.
40. Theilmeier, G., T. Lenaerts, C. Remacle, D. Collen, J. Vermylen, and M. F. Hoylaerts. 1999. Circulating activated platelets assist THP-1 monocytoid/endothelial cell interaction under shear stress. *Blood* 94: 2725–2734.
41. O'Brien, M., E. Montenont, L. Hu, M. A. Nardi, V. Valdes, M. Merolla, G. Gettenberg, K. Cavanagh, J. A. Aberg, N. Bhardwaj, and J. S. Berger. 2013. Aspirin attenuates platelet activation and immune activation in HIV-1-infected subjects on antiretroviral therapy: a pilot study. *J. Acquir. Immune Defic. Syndr.* 63: 280–288.
42. Gremmel, T., R. B. Eslam, R. Koppensteiner, I. M. Lang, and S. Panzer. 2013. Prasugrel reduces agonists' inducible platelet activation and leukocyte-platelet interaction more efficiently than clopidogrel. *Cardiovasc. Ther.* 31: e40–e45.
43. Schifitto, G., D. R. Peterson, J. Zhong, H. Ni, K. Cruttenden, M. Gaugh, H. E. Gendelman, M. Boska, and H. Gelbard. 2006. Valproic acid adjunctive therapy for HIV-associated cognitive impairment: a first report. *Neurology* 66: 919–921.
44. Islam, F. M., J. Wu, J. Jansson, and D. P. Wilson. 2012. Relative risk of cardiovascular disease among people living with HIV: a systematic review and meta-analysis. *HIV Med.* 13: 453–468.
45. Palella, F. J., Jr., and J. P. Phair. 2011. Cardiovascular disease in HIV infection. *Curr. Opin. HIV AIDS* 6: 266–271.
46. Ingersoll, M. A., R. Spanbroek, C. Lottaz, E. L. Gautier, M. Frankenberger, R. Hoffmann, R. Lang, M. Haniffa, M. Collin, F. Tacke, et al. 2010. Comparison

of gene expression profiles between human and mouse monocyte subsets. *Blood* 115: e10–e19.
47. Schulz, C., M. L. von Brühl, V. Barocke, P. Cullen, K. Mayer, R. Okrojek, A. Steinhart, Z. Ahmad, E. Kremmer, B. Nieswandt, et al. 2011. EMMPRIN (CD147/basigin) mediates platelet-monocyte interactions in vivo and augments monocyte recruitment to the vascular wall. *J. Thromb. Haemost.* 9: 1007–1019.
48. Postea, O., E. M. Vasina, S. Cauwenberghs, D. Projahn, E. A. Liehn, D. Lievens, W. Theelen, B. K. Kramp, E. D. Butoi, O. Soehnlein, et al. 2012. Contribution of platelet CX(3)CR1 to platelet-monocyte complex formation and vascular recruitment during hyperlipidemia. *Arterioscler. Thromb. Vasc. Biol.* 32: 1186–1193.
49. Laidlaw, T. M., M. S. Kidder, N. Bhattacharyya, W. Xing, S. Shen, G. L. Milne, M. C. Castells, H. Chhay, and J. A. Boyce. 2012. Cysteinyl leukotriene overproduction in aspirin-exacerbated respiratory disease is driven by platelet-adherent leukocytes. *Blood* 119: 3790–3798.
50. Pitchford, S. C., S. Momi, S. Baglioni, L. Casali, S. Giannini, R. Rossi, C. P. Page, and P. Gresele. 2008. Allergen induces the migration of platelets to lung tissue in allergic asthma. *Am. J. Respir. Crit. Care Med.* 177: 604–612.
51. van Gils, J. M., P. A. da Costa Martins, A. Mol, P. L. Hordijk, and J. J. Zwaginga. 2008. Transendothelial migration drives dissociation of plateletmonocyte complexes. *Thromb. Haemost.* 100: 271–279.